

Ab initio study of the electronic structure of manganese carbideApostolos Kalemos and Thom H. Dunning, Jr.^{a)}*Department of Chemistry, School of Chemical Sciences, University of Illinois at Urbana-Champaign, Urbana, Illinois 61801*

Aristides Mavridis

Laboratory of Physical Chemistry, Department of Chemistry, National and Kapodistrian University of Athens, P.O. Box 64 004, Zografou, Athens, 157 10, Greece

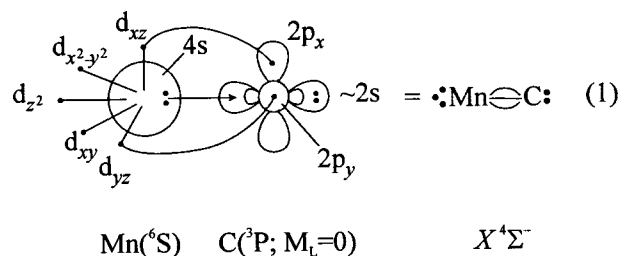
(Received 29 November 2005; accepted 8 February 2006; published online 19 April 2006)

We report electronic structure calculations on 13 states of the experimentally unknown manganese carbide (MnC) using standard multireference configuration interaction (MRCI) methods coupled with high quality basis sets. For all states considered we have constructed full potential energy curves and calculated zero point energies. The X state, correlating to ground state atoms, is of $4\Sigma^-$ symmetry featuring three bonds, with a recommended dissociation energy of $D_0=70.0$ kcal/mol and $r_e=1.640$ Å. The first and second excited states, which also correlate to ground state atoms, are of $6\Sigma^-$ and $8\Sigma^-$ symmetry, respectively, and lie 17.7 and 28.2 kcal/mol above the X state at the MRCI level of theory. © 2006 American Institute of Physics. [DOI: 10.1063/1.2181972]

I. INTRODUCTION

Aiming towards a comprehensive characterization of the electronic structure of the $3d$ -transition metal diatomic carbides and their cations MC and MC^+ , $M=Sc$,^{1(a)} (Sc^+),^{1(b),1(c)} Ti [Ref. 1(d)] (Ti^+),^{1(b),1(c)} V [Ref. 1(e)] (V^+),^{1(c),1(f)} Cr [Ref. 1(g)] (Cr^+),^{1(c),1(f)} Fe [Refs. 1(h)–1(j)] (Fe^+),^{1(k)} Co,^{1(l)} and Zn,^{1(m),1(n)} we report high level *ab initio* results for the ground and several excited states of manganese carbide (MnC). The existing theoretical literature on MnC is exhausted to a single article by Gutsev *et al.*,² who studied the ground states of all $MC^{0,\pm}$ and $MO^{0,\pm}$ species ($M=Sc-Zn$) using density functional theory (DFT). They identified the X state of MnC as of $4\Sigma^-$ symmetry with $r_e=1.606-1.699$ Å, dissociation energy $D_0=3.07-4.65$ eV, and dipole moment $\mu_e=2.75-3.00$ D, depending on the functional used. As far as we know no experimental data are available for MnC.

A state of $4\Sigma^-$ symmetry results naturally from the interaction of the ground state atoms as pictured clearly in valence-bond-Lewis (vbL) diagram 1.



The above diagram conforms also to the bonding pattern of the X states of both VC [Ref. 1(e)] and CrC [Ref. 1(g)] carbides. The $X^3\Sigma^-$ state of CrC arises by adding an electron to the δ orbital of the $X^2\Delta$ state of VC, while the $4\Sigma^-$ state of MnC is obtained by adding an electron to a σ orbital of the $X^3\Sigma^-$ state of CrC. It is interesting to note at this point that

the $X^3\Delta$ state of FeC [Ref. 1(h)] can be formed from the $X^4\Sigma^-$ state of MnC by adding one electron to one of the singly occupied δ_+ (or δ_-) orbitals. By doubly occupying the remaining d_δ orbital we obtain the $X^2\Sigma^+$ state of CoC [Ref. 1(l)] while a double occupancy of the last singly occupied orbital of σ type gives rise to the $X^1\Sigma^+$ of NiC.²

In the present work we examine by multireference variational methods all molecular states correlating to the $Mn(^6S)+[C(^3P),C(^1D)]$ atom limit, three states which correlate to the $Mn(^8P)+C(^3P)$ limit, and one state related to the $Mn(^6P)+C(^3P)$ limit, i.e., a total of 13 molecular states. Full potential energy curves (PEC) have been constructed for all states studied and standard spectroscopic constants have been calculated from the computed adiabatic potential energy curves.

II. METHODS

For the Mn atom the newly developed correlation consistent cc-pVQZ (22s18p11d3f2g1h) and cc-pwCVQZ (24s20p13d4f3g3h) basis sets of Balabanov and Peterson³ were employed; for the C atom the regular cc-pVQZ (12s6p3d2f1g) set by Dunning⁴ was used. Both sets were generally contracted to $[8s7p5d3f2g1h(10s9p7d4f3g2h)/Mn \ 5s4p3d2f1g/C]$ for the valence (core-valence) calculations. The zeroth-order wave functions are of the complete active space self-consistent-field (CASSCF) type and are formed by distributing the 11 valence electrons among 13 orbitals correlating to the (4s, 4p, 3d) atomic orbitals of Mn and the (2s, 2p) orbitals of C.

Additional electron correlation was introduced by including single+double excitations out of the zeroth-order space [CASSCF+1+2=multireference configuration interaction (MRCI)]. The size of the CI expansions range from $\sim 344 \times 10^6$ ($8\Sigma^-$ and 8Π states) to $\sim 1.4 \times 10^9$ configurations (for all the remaining states), internally contracted to about 3.8×10^6 ($8\Sigma^-$ and 8Π states) and $17-38 \times 10^6$ configura-

^{a)}Electronic mail: tdunning@ncsa.uiuc.edu

TABLE I. Total energies E (hartree) of the Mn ${}^6S(4s^23d^5)$ and C ${}^3P(2s^22p^2)$ states along with energy splittings ΔE (eV) of the Mn 6D , 8P , and 6P and C 1D terms, respectively, using a variety of electronic structure methods.

Mn				
Method ^a	$-E({}^6S)$	$\Delta E({}^6D \leftarrow {}^6S)$	$\Delta E({}^8P \leftarrow {}^6S)$	$\Delta E({}^6P \leftarrow {}^6S)$
CISD	1150.003 693	2.403	1.947	2.754
CISD+ Q	1150.013 75	2.384	2.135	2.905
CISD+DKH	1157.513 129	2.612	2.006	2.838
CISD+DKH+ Q	1157.523 28	2.585	2.195	2.987
C-CISD ^b	1150.396 090	2.154	1.711	2.609
C-CISD+ Q ^b	1150.434 23	2.078	1.972	2.821
C-CISD+DKH ^b	1157.906 035	2.383	1.774	2.702
C-CISD+DKH+ Q ^b	1157.944 510	2.315	2.041	2.918
MRCI	1150.10 860	2.520		
MRCI+ Q	1150.014 31	2.334		
MRCI+DKH	1157.520 336	2.725		
MRCI+DKH+ Q	1157.523 92	2.532		
C-MRCI ^b	1157.413 140	2.516		
C-MRCI+ Q ^b	1157.443 35	2.248		
C-MRCI+DKH ^b	1157.923 006	2.728		
C-MRCI+DKH+ Q ^b	1157.953 49	2.458		
Expt.	—	2.145	2.303	3.074

C		
Method	$-E({}^3P)$	$\Delta E({}^1D \leftarrow {}^3P)$
MRCI	37.784 932	1.275
MRCI+ Q	37.787 92	1.253
MRCI+DKH	37.799 928	1.275
MRCI+DKH+ Q	37.802 90	1.252
Expt.	—	1.260

^a+ Q and DKH refers to Davidson correction and second-order Douglas-Kroll-Hess scalar relativistic corrections, respectively. MRCI(Mn)=CASSCF($7e^-/4s, 4p, 3d$)+1+2, MRCI(C)=CASSCF($4e^-/2s, 2p$)+1+2.

^bThe $3s^23p^6$ semicore electrons of Mn are included in the CI procedure.

tions. For the $X^4\Sigma^-$ state, scalar relativistic effects were taken into account through the second-order Douglas-Kroll-Hess (DKH2) approximation⁵ by using the suggested contracted basis sets for both atoms.³ For all calculations the MOLPRO 2002.6 (Ref. 6) suite of programs was used.

III. RESULTS AND DISCUSSION

Table I presents total energies and splittings of the low-lying atomic states of the Mn and C atoms in a variety of methods. Note that the Mn 8P state is calculated in reverse order than the experimental findings⁷ with respect to the 6D term at all levels of theory. Table II summarizes our numerical results, whereas potential energy curves for all states are displayed in Fig. 1.

A. $X^4\Sigma^-$, $1^6\Sigma^-$, and $2^8\Sigma^-$ states

The ground state is of ${}^4\Sigma^-$ symmetry and dissociates to the ground state fragments: Mn($4s^23d^5, {}^6S$) + C($2s^22p^2, {}^3P; M_L=0$). The two atoms are held together by a σ and two π bonds while the electrons in the three non-bonding (“spectator”), singly occupied orbitals, two of $\delta-$ ($3d_{x^2-y^2}, 3d_{xy}$) and one of σ symmetry, define the spin and spatial symmetries of the molecule. The electronic arrangement can be synopsised by the vbL diagram 1.

The configuration with the largest coefficient at equilibrium is $|X^4\Sigma^- \rangle \cong 0.70 |(\text{core})^{20} 1\sigma^2 2\sigma^2 3\sigma^1 1\delta_+^1 1\pi_x^2 1\pi_y^2 1\delta_-^1 \rangle$ with corresponding Mulliken CASSCF atomic distributions (Mn/C),

$$4s^{0.84} 4p_z^{0.38} 3d_{z^2}^{1.14} 4p_x^{0.03} 3d_{xz}^{1.14} 4p_y^{0.03} 3d_{yz}^{1.14} 3d_{x^2-y^2}^{1.0} 3d_{xy}^{1.0} / 2s^{1.74} 2p_z^{0.88} 2p_x^{0.82} 2p_y^{0.82}.$$

The above imply the formation of a σ -dative bond by the transfer of about $0.7e^-$ from the $4s4p_z$ hybrid of Mn to the initially empty $2p_z$ C orbital, whereas the formation of two π bonds gives rise to a transfer of $0.4e^-$ from C to Mn; in total, about $0.3e^-$ migrate from Mn to C. A dissociation energy of $D_e=64.58(66.7)$ kcal/mol and equilibrium distance of $r_e=1.686(1.681)$ Å are obtained at the MRCI(+ Q) level of theory. Correcting for the zero point energy [$G(0)$] and basis set superposition error (BSSE), we obtain

$$\begin{aligned} D_0(+Q) &= D_e(+Q) - G(0)(+Q) + \text{BSSE}(+Q) \\ &= 64.58(66.7) - 0.86(0.90) - 0.39(0.42) \\ &= 63.33(65.4) \text{ kcal/mol.} \end{aligned}$$

Including scalar relativistic effects through the DKH2 approximation, we obtain $D_e+\text{rel}(+Q)=63.82(65.9)$ kcal/mol at $r_e=1.683(1.678)$ Å. Correcting for $G(0)$ and BSSE, we predict

TABLE II. Total MRCI energies E_e (hartree), bond distances r_e (Å), dissociation energies D_e (kcal/mol), zero point energies $G(0)$ (cm⁻¹), dipole moments μ (D), and energy gaps T_e (kcal/mol) of all MnC states presently studied, in ascending energy order. values in parenthesis refer to MRCI+Davidson correction.

Stste	$-E_e$	r_e	D_e	$G(0)$	$\langle\mu\rangle/\mu_{\text{FF}}^a$	T_e
$X^4\Sigma^-$	1187.893 01	1.686	64.58	299.80	1.96/2.35	0.0
	(1187.907 4)	(1.681)	(66.7)	(313.6)		(0.0)
$1^6\Sigma^-$	1187.864 76	1.965	46.85	256.24	2.29/2.65	17.73
	(1187.878 0)	(1.948)	(48.2)	(256.4)		(18.5)
$2^8\Sigma^-$	1187.848 00	2.093	36.33	255.43	2.45/2.75	28.25
	(1187.860 1)	(2.086)	(37.0)	(256.2)		(29.7)
$3^6\Sigma^-$	1187.824 55	2.006	68.74	282.03	1.68/2.05	42.96
	(1187.838 1)	(1.995)	(72.0)	(284.2)		(43.5)
$4^4\Pi$	1187.823 68	1.617	21.21	430.12	4.86/5.21	43.50
	(1187.841 3)	(1.618)	(25.2)	(435.2)		(41.5)
$5^6\Delta$	1187.817 76	1.929	47.35	218.44	2.99/3.29	47.22
	(1187.833 3)	(1.910)	(49.5)	(228.7)		(46.2)
$6^6\Pi$	1187.809 72	1.738	12.90	351.99	3.0	52.27
	(1187.828 2)	(1.734)	(17.1)	(391.5)		(49.7)
		Local minimum				
	1187.806 3	2.147		214.16		
	(1187.821 4)	(2.132)		339.2		
$7^4\Pi$	1187.805 36	1.792	78.46	533.03	1.98	55.0
$8^8\Pi$	1187.802 98	2.271	8.22	191.67	2.22/2.23	56.49
	(1187.816 5)	(2.274)	(9.6)	(179.9)		(57.1)
$9^6\Sigma^+$	1187.798 03	1.952	34.74	230.61	3.06/3.38	59.60
	(1187.812 5)	(1.931)	(36.2)	(233.4)		(59.6)
$10^6\Pi$	1187.787 71	1.930	29.17	567.94	2.85	66.08
	(1187.805 1)	(1.934)	(31.9)	(461.5)		(64.2)
		Local minimum				
	1187.786 54	2.171		252.77		
$11^6\Pi$	1187.782 25	2.021	44.87	478.14	1.7	69.51
	(1187.799 7)	(2.012)	(48.7)	(448.5)		(67.6)
$12^8\Pi$	1187.775 48	2.015	40.53	421.58	3.57/4.07	73.75
	(1187.791 9)	(2.015)	(43.8)	(427.6)		(72.5)

^aDipole moments $\langle\mu\rangle$ are obtained as expectation values; μ_{FF} through the finite field method.

$$\begin{aligned}
 D_0(+Q) &= D_e + \text{rel}(+Q) - G(0)_{\text{rel}}(+Q) + \text{BSSE}(+Q) \\
 &= 63.82(65.9) - 0.87(0.93) - 0.39(0.42) \\
 &= 62.56(64.6) \text{ kcal/mol.}
 \end{aligned}$$

In order to perform corresponding MRCI calculations but including the semicore Mn($3s^23p^6$) electrons, we were forced, because of the extremely large number of ensuing configurations, to remove the three Mn($4p$) orbitals from the active space of the zeroth-order (CASSCF) reference function. Within this space our valence MRCI+ Q results are $D_e=65.91(66.5)$ kcal/mol at $r_e=1.671(1.667)$ Å as contrasted with $D_e=64.58(66.7)$ kcal/mol and $r_e=1.686(1.681)$ Å. Including core-valence correlation effects we get $D_e=67.66(71.8)$ kcal/mol and $r_e=1.648(1.641)$ Å. Further correcting now for relativity, $G(0)$ and BSSE, we obtain

$$\begin{aligned}
 D_0(+Q) &= D_e + \text{rel}(+Q) - G(0)_{\text{rel}}(+Q) + \text{BSSE}(+Q) \\
 &= 68.18(71.3) - 1.06(1.17) - 0.39(0.42) \\
 &= 66.73(69.7) \text{ kcal/mol}
 \end{aligned}$$

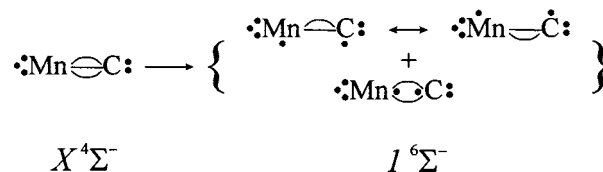
and $r_e=1.647(1.639)$ Å. Therefore, our “best” r_e and D_0 values for the $X^4\Sigma^-$ state of MnC are 1.640 Å and 70 kcal/mol,

respectively, an increase of less than 5 kcal/mol as compared with the plain MRCI D_0 value.

The first excited state of MnC is of $6^6\Sigma^-$ symmetry and lies 17.73(18.5) kcal/mol above the X state at the MRCI(+ Q) level. The interpretation of the wave function’s character at equilibrium is rather difficult due to its dispersion over many CFs. For instance, the sum of the square of the first ten variational coefficients of the leading CFs does not exceed 0.72, the first three of which are given below:

$$\begin{aligned}
 |1^6\Sigma^- \rangle &\cong -0.38|1\sigma^2 2\sigma^2 3\sigma^1 1\delta_+^1 \rangle \\
 &\quad \times (1\pi_x^2 1\pi_y^1 2\pi_y^1 + 1\pi_x^1 2\pi_x^1 1\pi_y^2) 1\delta_-^1 \rangle \\
 &\quad + 0.28|1\sigma^2 2\sigma^1 3\sigma^1 1\delta_+^1 4\sigma^1 1\pi_x^2 1\pi_y^1 1\delta_-^1 \rangle.
 \end{aligned}$$

However, closer examination and comparison to the $X^4\Sigma^-$ state reveal a simple and quite interesting bonding pattern described by the following structure:



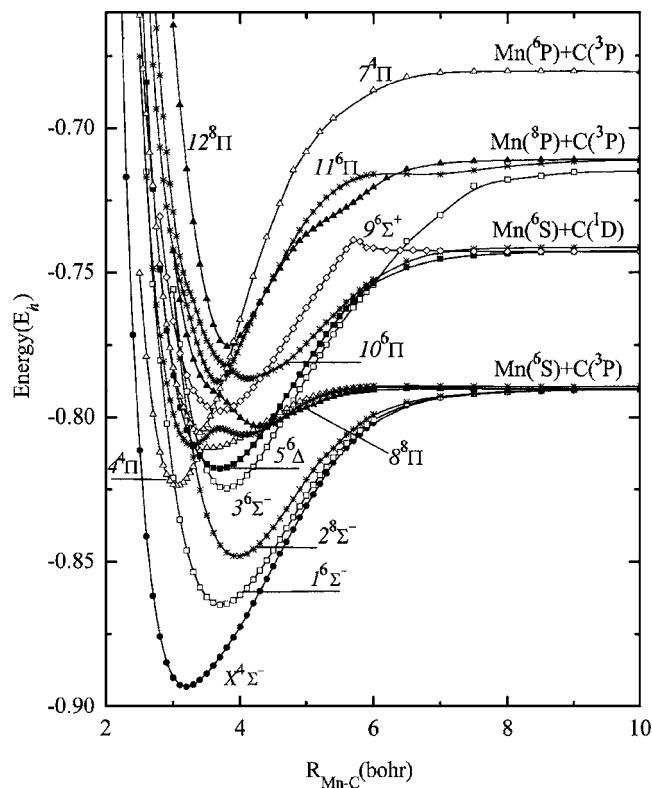


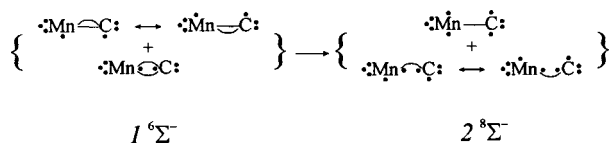
FIG. 1. Potential energy curves of 13 MnC states at the MRCI level of theory. Energies have been shifted by $+1187.0E_h$.

The $1^6\Sigma^-$ state can be described as a “mixture” of two major double bonded structures: a (σ, π) and (π, π) one at the expense of a π and σ bond, respectively, of the $X^4\Sigma^-$ state.

The second excited state, which also correlates to the ground state fragments, $\text{Mn}(^6S) + \text{C}(^3P; M_L=0)$, lies $T_e = 28.25(29.7)$ kcal/mol higher and is a high spin octet state $2^8\Sigma^-$. The main CASSCF equilibrium configurations for this state,

$$|2^8\Sigma^-\rangle \cong 0.56|1\sigma^2 2\sigma^2 3\sigma^1 1\delta_x^1 1\pi_x^1 2\pi_x^1 \pi_y^1 2\pi_y^1 1\delta_x^1\rangle \\ + 0.38|1\sigma^2 2\sigma^1 3\sigma^1 1\delta_x^1 4\sigma^1 (1\pi_x^1 2\pi_x^1 \pi_y^2 \\ + 1\pi_x^2 1\pi_y^1 2\pi_y^1) 1\delta_x^1\rangle,$$

appear rather puzzling *vis-à-vis* the interpretation of the chemical bond, but when considered along with those of the $X^4\Sigma^-$ and $1^6\Sigma^-$ states they reveal a rather “simple” bonding picture visualized by the following Lewis structures.



This state is characterized as a σ and π bonded system and can be derived directly from the $1^6\Sigma^-$ state by breaking a π bond from its (σ, π) and (π, π) major components. The parental state $X^4\Sigma^-$, a (σ, π, π) bonded structure, becomes sequentially a $(\sigma, \pi)/(\pi, \pi)$ state ($1^6\Sigma^-$), and finally a σ/π system state ($2^8\Sigma^-$). Moving from $X^4\Sigma^-$ through $1^6\Sigma^-$ to $2^8\Sigma^-$, the binding energies decrease monotonically followed

by a “logical” increase of the corresponding bond distances: $D_e = 64.58(66.7)$, $46.85(48.2)$, and $36.33(37.0)$ kcal/mol, and $r_e = 1.686(1.681)$, $1.965(1.948)$, and $2.093(2.086)$ Å, respectively, at the MRCI(+ Q) level of theory.

B. $3^6\Sigma^-$ state

The next state in ascending energy order is (formally) of $6\Sigma^-$ symmetry lying $42.96(43.5)$ kcal/mol above the X state. It is practically degenerate with a rival state of 4Π symmetry at $43.50(41.5)$ kcal/mol with respect to the ground state. The intense multiconfigurational character of $3^6\Sigma^-$, as evidenced by a dispersion of the MRCI coefficients over many configurations, prohibits any discussion of its bonding features, and consequently no simple vbL structures can be drawn.

The binding energy with respect to the dissociation channel $\text{Mn}(4s^1 4p^1 3d^5; ^8P) + \text{C}(^3P)$ is $D_e = 68.74(72.0)$ kcal/mol with $r_e = 2.006(1.995)$ Å at the MRCI(+ Q) level of theory. However, it should be noted at this point that $\text{Mn}(^8P) + \text{C}(^3P)$ is not the adiabatic dissociation limit $\text{Mn}(^6D) + \text{C}(^3P)$, which lies below the $\text{Mn}(^8P) + \text{C}(^3P)$ channel with an experimental energy splitting of $\Delta E(^8P \leftarrow ^6D) = 0.158$ eV.⁷ This “anomaly” is due to the better description of the $\text{Mn}(^8P)$ state than the $\text{Mn}(4s^1 3d^6; ^6D)$ one at all levels of calculation, therefore predicting the 8P state lower than the 6D by 0.378 eV at the MRCI level. Thus, with respect to the 6D the dissociation energy should be increased by about 0.378 eV or $D_e \cong 77.5$ kcal/mol. Although our wave function does not conform to the correct dissociation limit, we believe that it behaves reasonably well around equilibrium and includes the necessary ingredients for a balanced and physically acceptable description.

C. $4^4\Pi$ and $7^4\Pi$ states

These two 4Π states interact at ~ 3.4 bohr as depicted nicely in Fig. 1. The $4^4\Pi$ curve stems from the ground state atoms maintaining this character up to 3.5 bohr where an avoided crossing with the incoming $7^4\Pi$ state is realized. The most characteristic feature of this interaction is the introduction of $4p$ metallic character through the $\text{Mn}(4s^1 4p^1 3d^5; ^6P)$ as evidenced by its ($7^4\Pi$) dissociation path, i.e., $\text{Mn}(^6P) + \text{C}(^3P)$. The leading configuration of the $4^4\Pi$ state, along with its Mulliken CASSCF atomic distributions, is

$$|4^4\Pi\rangle \cong 0.74|1\sigma^2 2\sigma^2 1\delta_x^1 1\pi_x^2 1\pi_y^2 2\pi_y^1 1\delta_x^1\rangle \\ 4s^{0.28} 4p_z^{0.12} 3d_{z^2}^{1.22} 4p_x^{0.04} 3d_{xz}^{1.15} 4p_y^{0.70} 3d_{yz}^{1.21} 3d_{x^2-y^2}^{1.0} 3d_{xy}^{1.0} \\ |2s^{1.62} 2p_z^{0.74} 2p_x^{0.79} 2p_y^{1.07}\rangle.$$

This clearly indicates that the Mn atom is in the excited 6P state. Notice, that the minimum of the $7^4\Pi$ is located at the avoided crossing with the $4^4\Pi$ state. A second avoided crossing at 2.75 bohr is observed between the $7^4\Pi$ and another 4Π not presently studied.

D. 5 ${}^6\Delta$ and 9 ${}^6\Sigma^+$ states

Both states correlate to $\text{Mn}(4s^2 3d^5; {}^6S) + \text{C}(2s^2 2p^2; {}^1D)$. Due to the spherical symmetry of the metal atom the $\Lambda=2$ or 0^+ symmetry of the titled states is the result of the different vector components of the C atom,

$$|{}^1D; M_L = \pm 2\rangle_{A_1} = (1/\sqrt{2})|2s^2(2p_x^2 - 2p_y^2)\rangle,$$

and

$$|{}^1D; M_L = 0\rangle = (1/\sqrt{6})\{2|2s^2 2p_z^2\rangle - |2s^2 2p_x^2\rangle - |2s^2 2p_y^2\rangle\}.$$

At equilibrium they share the same binding characteristics conforming to the main configurations and CASSCF Mulliken populations,

$$|5 {}^6\Delta\rangle \cong 0.43|1\sigma^2 2\sigma^2 1\delta_+^1 3\sigma^1(1\pi_x^2 2\pi_x^1 1\pi_y^1 - 1\pi_x^1 1\pi_y^2 2\pi_y^1)1\delta_-^1\rangle$$

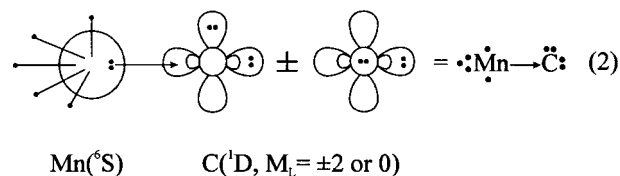
$$4s^{0.93} 4p_z^{0.23} 3d_{z^2}^{1.05} 4p_x^{0.15} 3d_{xz}^{1.04} 4p_y^{0.15} 3d_{yz}^{1.04} 3d_{x^2-y^2}^{1.0} 3d_{xy}^{1.0} \\ /2s^{1.82} 2p_z^{0.95} 2p_x^{0.80} 2p_y^{0.80},$$

and

$$|9 {}^6\Sigma^+\rangle \cong 0.44|1\sigma^2 2\sigma^2 1\delta_+^1 3\sigma^1 \\ \times (1\pi_x^2 2\pi_x^1 1\pi_y^1 + 1\pi_x^1 1\pi_y^2 2\pi_y^1)1\delta_-^1\rangle$$

$$4s^{0.91} 4p_z^{0.21} 3d_{z^2}^{1.04} 4p_x^{0.18} 3d_{xz}^{1.04} 4p_y^{0.18} 3d_{yz}^{1.04} 3d_{x^2-y^2}^{1.0} 3d_{xy}^{1.0} \\ /2s^{1.80} 2p_z^{0.95} 2p_x^{0.81} 2p_y^{0.82}.$$

The associated vbL diagram is shown below.



The two atoms interact attractively through a single σ bond and not via a σ and π as perhaps conveyed misleadingly by the CASSCF configurations. The D_e (kcal/mol) and r_e (Å) values are 47.35 (49.5), 34.74 (36.2) and 1.929 (1.910), 1.952 (1.931) for the 5 ${}^6\Delta$ and 9 ${}^6\Sigma^+$ states, respectively, at the MRCI (+Q) level. The almost identical dipole moments, 2.99 (5 ${}^6\Delta$) and 3.06 (9 ${}^6\Sigma^+$) D, are also indicative of their similar electronic distributions.

Following the evolution of the bond formation along the potential energy curves of both states, it is easily inferred that in the case of the 5 ${}^6\Delta$ state, the character at infinity is maintained along the potential curve, while in the case of the 9 ${}^6\Sigma^+$ the repulsive $|2s^2 2p_z^2\rangle$ component of the $\text{C}({}^1D; M_L=0)$ term is gradually decreased up to around 6.2 bohrs projected in the hump of its potential energy curve (Fig. 1). By reasons of symmetry this “unclogging” interaction should be provided by a ${}^6\Sigma^+$ state resulting from the $\text{C}({}^1S)$ atomic state.

E. 6 ${}^6\Pi$, 10 ${}^6\Pi$, and 11 ${}^6\Pi$ states

These states are discussed together because of their intertwined behavior for several regions of the Mn–C distance. The 6 ${}^6\Pi$ results from the interaction of the ground state atoms, $\text{Mn}({}^6S) + \text{C}({}^3P)$, whereas the 10 ${}^6\Pi$ state correlates to

$\text{Mn}({}^6S) + \text{C}({}^1D)$. The 11 ${}^6\Pi$ is expected to dissociate adiabatically to $\text{Mn}(4s^1 3d^6; {}^6D) + \text{C}({}^3P)$, but due to its poor description at all levels of theory, this channel lies above the experimentally higher $\text{Mn}(4s^1 4p^1 3d^5; {}^8P)$ atomic term, which also gives rise to ${}^6\Pi$ states. Consequently, and incorrectly, this state arises from the $\text{Mn}({}^8P) + \text{C}({}^3P)$ separated atom limit. We believe, however, that close to equilibrium the natural content of the wave functions is adequately described.

Notwithstanding the intense multiconfigurational, and rather blurry character of these sextet Π states, we will try to comment upon their most important features. The local minimum (*l*) of the 6 ${}^6\Pi$ state is dominated by a configuration that reflects its character at infinity, i.e.,

$$|6 {}^6\Pi\rangle_l \cong 0.48|1\sigma^2 2\sigma^2 3\sigma^1 1\delta_+^1 4\sigma^1 1\pi_x^2 1\pi_y^1 1\delta_-^1\rangle,$$

and

$$4s^{1.05} 4p_z^{0.41} 3d_{z^2}^{1.03} 4p_x^{0.09} 3d_{xz}^{1.04} 4p_y^{0.02} 3d_{yz}^{1.0} 3d_{x^2-y^2}^{1.0} 3d_{xy}^{1.0} \\ /2s^{1.87} 2p_z^{1.37} 2p_x^{0.87} 2p_y^{0.21},$$

while its global minimum (*g*), past an avoided crossing at around 3.7 bohr, is dominated by the character of the third ${}^6\Pi$ (11 ${}^6\Pi$) state that carries the memory of the $\text{Mn}(4s^1 4p^1 3d^5; {}^8P; M_L = \pm 1)$ atomic term,

$$|6 {}^6\Pi\rangle_g \cong 0.72|1\sigma^2 2\sigma^1 3\sigma^1 1\delta_+^1 1\pi_x^2 1\pi_y^2 2\pi_y^1 1\delta_-^1\rangle,$$

and

$$4s^{0.78} 4p_z^{0.17} 3d_{z^2}^{0.93} 4p_x^{0.07} 3d_{xz}^{1.10} 4p_y^{0.41} 3d_{yz}^{1.19} 3d_{x^2-y^2}^{1.0} 3d_{xy}^{1.0} \\ /2s^{1.69} 2p_z^{0.48} 2p_x^{0.82} 2p_y^{1.31}.$$

The 10 ${}^6\Pi$ and 11 ${}^6\Pi$ states are more entangled as evidenced by the potential energy curves of Fig. 1 and, consequently, their character is difficult to be analyzed. The local (*l*) minimum of the 10 ${}^6\Pi$ state is

$$|10 {}^6\Pi\rangle_l \cong 0.48|1\sigma^2 2\sigma^2 3\sigma^2 1\delta_+^1 1\pi_x^2 2\pi_x^1 1\pi_y^1 1\delta_-^1\rangle \\ + 0.41|1\sigma^2 2\sigma^2 3\sigma^1 1\delta_+^1 4\sigma^1 1\pi_x^2 2\pi_x^1 1\pi_y^1 1\delta_-^1\rangle \\ - 0.29|1\sigma^2 2\sigma^2 3\sigma^1 1\delta_+^1 4\sigma^1 1\pi_x^2 2\pi_x^2 2\pi_y^1 1\delta_-^1\rangle \\ - 0.23|1\sigma^2 2\sigma^2 3\sigma^2 1\delta_+^1 1\pi_x^2 2\pi_x^1 2\pi_y^1 1\delta_-^1\rangle,$$

whereas its global (*g*) minimum is situated very close to an avoided crossing with the higher located 11 ${}^6\Pi$ state, and is a mixture of different bonding schemes:

$$|10 {}^6\Pi\rangle_g \cong 0.44|1\sigma^2 2\sigma^2 3\sigma^1 1\delta_+^1 4\sigma^1 1\pi_x^2 1\pi_y^1 1\delta_-^1\rangle \\ + 0.40|1\sigma^2 2\sigma^1 3\sigma^1 1\delta_+^1 1\pi_x^2 1\pi_y^2 2\pi_y^1 1\delta_-^1\rangle \\ - 0.24|1\sigma^2 2\sigma^2 3\sigma^1 1\delta_+^1 4\sigma^1 1\pi_x^2 2\pi_x^1 1\delta_-^1\rangle \\ + 0.21|1\sigma^2 2\sigma^2 3\sigma^2 1\delta_+^1 1\pi_x^2 2\pi_x^1 1\pi_y^1 1\delta_-^1\rangle.$$

This makes its “chemical” interpretation unwieldy. The last avoided crossing with the 11 ${}^6\Pi$ state is located around 3.1 bohr; past this point the two curves interchange their bonding character.

The case of the 11 ${}^6\Pi$ state is further complicated by the fact that its minimum is situated on the avoided crossing

with the previously discussed $10^6\Pi$. Its major components at the minimum convey a rather “fuzzy” situation,

$$\begin{aligned} |11^6\Pi\rangle \cong & 0.54|1\sigma^2 2\sigma^2 3\sigma^2 1\delta_+^1 1\pi_x^1 2\pi_x^1 1\pi_y^1 1\delta_-^1\rangle \\ & + 0.29|1\sigma^2 2\sigma^2 3\sigma^1 1\delta_+^1 4\bar{\sigma}^1 1\pi_x^1 2\pi_x^1 1\pi_y^1 1\delta_-^1\rangle \\ & - 0.22|1\sigma^2 2\sigma^2 3\sigma^1 1\delta_+^1 4\sigma^1 1\bar{\pi}_x^1 2\pi_x^1 1\pi_y^1 1\delta_-^1\rangle \\ & - 0.22|1\sigma^2 2\sigma^2 3\sigma^1 1\delta_+^1 4\bar{\sigma}^1 1\pi_x^1 2\pi_x^1 2\pi_y^1 1\delta_-^1\rangle. \end{aligned}$$

F. $8^8\Pi$ and $12^8\Pi$ states

The $8^8\Pi$ state dissociates to ground state fragments, i.e., $\text{Mn}(^6S) + \text{C}(^3P; M_L = \pm 1)$. Its equilibrium CASSCF configuration

$$|8^8\Pi\rangle \cong 0.95|1\sigma^2 2\sigma^2 3\sigma^1 1\delta_+^1 4\sigma^1 1\pi_x^1 2\pi_x^1 1\pi_y^1 1\delta_-^1\rangle$$

reflects its parental character, which is, however, lost after an avoided crossing at around 3.8 bohr with the $12^8\Pi$ state. By comparing the $8^8\Pi$ with the main configuration of the $|6^6\Pi\rangle_l$ state, we observe that it results from the latter by breaking a π bond.

The $12^8\Pi$ state, the highest of all states studied here, dissociates to $\text{Mn}(^8P) + \text{C}(^3P)$, although its correct adiabatic limit is $\text{Mn}(^6D) + \text{C}(^3P)$. The 8P atomic term introduces $4p$ metallic character, which is evident both in its equilibrium configurations and in the $8^8\Pi$ state after the avoided crossing. The minimum, in the region of the interaction with the $8^8\Pi$ state, is a mixture of both bonding schemes,

$$\begin{aligned} |12^8\Pi\rangle \cong & 0.55|1\sigma^2 2\sigma^1 1\delta_+^1 3\sigma^1 1\pi_x^1 2\pi_x^1 1\pi_y^2 2\pi_y^1 1\delta_-^1\rangle \\ & - 0.49|1\sigma^2 2\sigma^2 1\delta_+^1 3\sigma^1 4\sigma^1 1\pi_x^1 2\pi_x^1 1\pi_y^2 1\delta_-^1\rangle, \end{aligned}$$

hampering a chemical interpretation along the traditional path.

IV. SUMMARY

We have reported, for the first time, high level *ab initio* results on 13 states of the experimentally unknown MnC. Most of the molecular states have intense multiconfigurational character, thus rendering MRCI the only suitable method to treat such complicated cases. The X state is of $^4\Sigma^-$ symmetry featuring three bonds: a σ and two π bonds with a suggested $D_0 = 70.0$ kcal/mol at $r_e = 1.640$ Å. All of states studied here are bound with respect to their dissociation limits and cover an energy range of 74 kcal/mol. Dipole moments have been calculated both as expectation values ($\langle\mu\rangle$) and by the finite field method (μ_{FF}); in all examined states $|\mu_{\text{FF}}| > |\langle\mu\rangle|$ by 0.3–0.4 D, and according to our experience [see also Refs. 1(i) and 1(j)], μ_{FF} values are to be trusted more than the $\langle\mu\rangle$ ones.

- ¹(a) A. Kalemos, A. Mavridis, and J. F. Harrison, *J. Phys. Chem. A* **105**, 755 (2001); (b) I. S. K. Kerkines and A. Mavridis, *J. Phys. Chem. A* **104**, 11777 (2000); (c) I. S. K. Kerkines and A. Mavridis, *Collect. Czech. Chem. Commun.* **68**, 387 (2003); (d) A. Kalemos and A. Mavridis, *J. Phys. Chem. A* **106**, 3905 (2002); (e) A. Kalemos, T. H. Dunning Jr., and A. Mavridis, *J. Chem. Phys.* **123**, 014301 (2005); (f) I. S. K. Kerkines and A. Mavridis, *Mol. Phys.* **102**, 2451 (2004); (g) A. Kalemos, T. H. Dunning Jr., and A. Mavridis, *J. Chem. Phys.* **123**, 014302 (2005); (h) D. Tzeli and A. Mavridis, *J. Chem. Phys.* **116**, 4901 (2002); (i) D. Tzeli and A. Mavridis, *J. Chem. Phys.* **118**, 4984 (2003); (j) D. Tzeli and A. Mavridis, *J. Chem. Phys.* **122**, 056101 (2005); (k) D. Tzeli and A. Mavridis, *J. Phys. Chem. A* **109**, 9249 (2005); (l) D. Tzeli and A. Mavridis (unpublished); (m) I. S. K. Kerkines, J. Pittner, P. Čársky, A. Mavridis, and I. Hubáč, *J. Chem. Phys.* **117**, 9733 (2002); (n) A. Tsouloucha, I. S. K. Kerkines, and A. Mavridis, *J. Phys. Chem. A* **107**, 6062 (2003).
- ²G. L. Gutsev, L. Andrews, and C. W. Bauschlicher Jr., *Theor. Chem. Acc.* **109**, 298 (2003).
- ³N. B. Balabanov and K. A. Peterson, *J. Chem. Phys.* **123**, 064107 (2005).
- ⁴T. H. Dunning Jr., *J. Chem. Phys.* **90**, 1007 (1989).
- ⁵M. Douglas and N. M. Kroll, *Ann. Phys. (N.Y.)* **82**, 89 (1974); B. A. Hess, *Phys. Rev. A* **32**, 756 (1985); B. A. Hess, *Phys. Rev. A* **33**, 3742 (1986).
- ⁶H.-I. Werner, P. J. Knowles, R. D. Amos *et al.*, MOLPRO, a package of *ab initio* programs, version 2002.6 (Birmingham, UK, 2002).
- ⁷C. E. Moore, *Atomic Energy Levels*, Natl. Bur. Stand. Ref. Data U.S. GPO, Ser., Natl. Bur. Stand. (U.S.) Circ. No. 35 (Washington, D.C., 1971), Vol. III.